

1. Introduction

1.1. Palaeoclimatology:

The oceans cover nearly 70% of the Earth's surface, which drive and regulate its total climate system. The climate encompasses complex and multitude interactions between atmosphere, hydrosphere, cryosphere, biosphere, and lithosphere. Such interactions on large scale may induce distinct changes in the global climate. The excess accumulation of greenhouse gases such as carbon dioxide and methane leading to modern climate warming greatly modify the Earth's climate system. The ENSO type of ocean-atmosphere coupled process modifies the global precipitation pattern. These climate features stand out as examples of the complex interactions between atmosphere and hydrosphere. In the 18th century James Hutton and Charles Lyell proposed principles of uniformitarianism considering '*present as key to the past*'; whereas the palaeoclimatologists endeavour to '*predict the future climate by looking in to the past-variations*'. Only when the causes of the past climate fluctuations are understood, it will be possible to anticipate or forecast climatic variations in the future (Bradley and Eddy, 1991). Our present knowledge of the past-Earth has indicated several alternating warm and cold periods particularly in the Pleistocene with amazing rhythm. Hence, the Pleistocene Period is rightly coined as the Great Ice Age. The ocean as a major player involved either in generating such climate variations or in feedback mechanism required for climatic oscillations, hence the oceanic response to the Earth's climate change although very complex has been distinct and measurable. Therefore, oceans provide most important and easily accessible repository for tracing the past climate records. Almost all changes in oceanic environment in response to climate variation could be traced within the seafloor itself. In that, the seafloor sediments faithfully record the changes in water column chemistry, biological activity, air-sea interaction, inter-oceanic overturning, land-ocean interaction, deep-water circulation etc.

Both regional- and global-scale climate changes have been attributed to the uneven heating of the planet by the solar radiation. In other words, Earth's radiation budget largely controls the climate. A steady state climate unchanged over a period should ideally represent well-balanced radiation budget of the Earth i.e., incoming solar radiation equals the outgoing radiations. This balance has fluctuated several times in the past resulting in cooling and warming of the climate, which are commonly known as glacial and interglacial periods respectively. Earth has experienced such dramatic climatic conditions during the last 2.7 million years. Within the late Quaternary itself (since ~1 Ma) there have been ten major cold (glacial) events separated by warm (interglacial) events known as climatic cycles. These climatic cycles are further punctuated by shorter time-span, moderately cold and warm events called stadial and interstadial respectively. The main effect of these glacial-interglacial climate cycles was extensive waxing and waning of the continental ice sheets resulting in fall and rise of the global sea level, which have further modified the continental and oceanic climate set-up. For instance, during the last glacial maximum (LGM) the global sea level was lowered by about 120 m as a result of global oceans losing large amount of freshwater, which was locked on the continents in the form of ice (Fairbank 1982; Shackleton and Opdyke, 1973). In fact, the climate must have been subjected to such changes on global-scale since the time earth has come into existence (~4.5 billions of years ago) as a part of its natural dynamics. The information related to those changes has been stored in different forms (proxies) on continents and in oceans (e.g., ~3.3 billion years old Banded Iron Formations and few thousand years old marine sediments). The time-scale of changes, which one could resolve depends upon the process involved in the genesis of particular proxy and the location of its formation. The shallow water corals, for example, may provide the information on yearly time-scale, but the deep abyssal oceanic sediment on thousands of years time-scale. The resolution also depends upon the sampling and measurement techniques. Recent studies of the Greenland

ice sheets have revealed astonishingly abrupt climatic oscillations with significant amplitude variations (Dansgaard et al., 1984; Oeschger et al., 1984), subsequently named after their discoverers as Dansgaard-Oeschger climate oscillations. The modern anthropogenic forcing on the climate change is an additional signal superimposed on the background of natural climate. It is possible to isolate anthropogenic or local effects from a composite record, if we subtract the natural effect with reasonable confidence. Therefore, it is important to learn about the variability in the past-climate to understand or predict the possible future changes. This highly intriguing, fascinating, and complex branch of earth sciences is termed as 'Palaeoclimatology'.

The Quaternary Period is the most important time in the geological history as far as the past climate variability is concerned, because it provides immediate past climate history based on which one can understand the present and anticipate future changes. In particular, the climate contrast between the Last Glacial Period (LGP: 24 Ka - 11 Ka) and the Holocene (11 Ka to Present) provides valuable information for projecting the future natural climate change. Additionally, the Holocene epoch forms the present day warm and humid climate cycle, while the LGP represents the immediate past cold and dry climate. This pattern of climate cycle has repeated in the past with amazing accuracy and resulted in distinct global as well as local responses in hydrosphere and biosphere. As the oceans host the largest volume of water and the organic production, is the most suitable candidate to trace the past climate. Therefore, the marine sediment has been the widely explored effective archive to study the palaeoclimate on different time scales depending upon the location of the study area. The atmosphere-hydrosphere coupled processes such as monsoon intensity, oceanic upwelling, biological productivity, and atmosphere-continent coupled processes such as dust flux, fluvial erosion etc in response to climate forcing could be understood using the marine sediments.

1.2. History of Ice Age:

The recognition and evolution of the Quaternary climate change has a history of more than two centuries. Today about 10% of the Earth's total land area is covered by glacier ice. Whereas, during the Pleistocene at several times as high as ~30 % of the land surface was covered with the ice and oceanic ice-sheets expanded to great extent resulting in overall cooling of the climate. In 1795, James Hutton suggested that the continental glaciers transported the erratic boulders of granite found in limestone of the Jura Mountains. In 1823, William Buckland, while describing the Quaternary Cave deposits, suggested that the northern Britain and several parts of the north Europe were covered by glacier ice in the past. Those thought provoking studies basically recognised the ice age. Geikie brothers in 1870s extensively described the glacial drifts and their work laid the foundation for the Quaternary ice age. Subsequently, alternating cold and warm events with well-defined rhythm were recognised in global marine sedimentary records spanning several thousands of years. Based on these records past climate models were developed and hypothesis were proposed. The most important of them was the *Orbital Theory* propounded by Milankovitch (1941), which recognized that the past glaciations were principally the function of variations in the Earth's orbital parameters resulting in varying distribution of solar radiance on its surface.

The revolution in Quaternary climate study took place in 1946 when Harold Urey demonstrated that the oxygen isotope ratios of planktonic foraminifera indicate the temperature of the seawater in which they lived. With each 1°C fall in ambient water temperature, the $\delta^{18}\text{O}$ of planktonic calcite was shown to increase by 0.2 ‰. Fluctuations in the oxygen isotopic ratios and major changes in the global climate were extensively studied by Emiliani (1955). The subsequent detailed investigations of $\delta^{18}\text{O}$ variations in the calcite tests of planktic and benthic foraminifera confirmed the temperature dependence of the oxygen isotopic ratio. Later studies by Olausson

(1965), Shackleton (1967), and Shackleton and Opdyke (1973) led to the conclusion that variations in the calcite- $\delta^{18}\text{O}$ with time reflected changes in the oceanic oxygen isotope composition caused mainly by the waxing and waning of the continental ice sheets that led to fall and rise of the global sea level. Fairbanks and Mathews (1978) estimated that 0.011 ‰ of $\delta^{18}\text{O}$ variation is associated with 1 m of sea-level change. With the evolution of oxygen isotopic studies of marine biogenic calcite, it has become unequivocally clear that, irrespective of the region the temporal records of both the planktic and benthic foraminifera $\delta^{18}\text{O}$ exhibited remarkable global similarity comprising major cold (glacial) and warm (interglacial) events repeating at ~100 ky (orbital eccentricity) frequency. At the outset this observation suggested that, a) the past variations in the climate have forced the global oceans' $\delta^{18}\text{O}$ to change accordingly, b) the record of such changes are preserved with remarkable fidelity in the calcite fossils on global scale, and c) the changes were the responses to orbital parameters. The first rigorous attempt to assess the orbital parameters forcing the past climate change was made by Hays et al. (1976). They concluded that most of the changes observed in marine sedimentary records were found to concentrate at frequencies closely corresponding to those expected from the orbital changes (e.g., ~100 kyr Eccentricity, ~41 kyr Obliquity, and ~21 kyr Precession periodicities recognised by Milankovitch). The accurate marine oxygen isotopic stages were defined based on the stacked oxygen isotope data of the foraminifer calcite and tuning the down-core isotope profiles to the solar insolation curve (Imbrie et al., 1984). This insolation-tuned sedimentary marine oxygen isotope profile widely known as the SPECMAP became the reference curve for the Quaternary chronology for demarcating the Marine Oxygen Isotope Stages (MIS). These stages were numbered serially from present warm Holocene period in to the past. Thus the odd numbers indicate the warm interglacial periods and the even numbers indicate cold glacial periods. Numerous other studies carried out using the sedimentary records

from the world oceans and regional seas subsequently confirmed the orbital theory of Quaternary climate change (see for examples Imbrie et al., 1984, Bassinot et al., 1994, Shackleton, 2000). In the past decade new discoveries were made using the Greenland ice-cores. Those ice-core studies have revealed that the past cyclic climate change was not solely on orbital frequencies but on much more rapid sub-orbital frequencies (Bond et al., 1993; Dansgaard et al., 1984; Heinrich, 1984; Oeschger et al., 1984). That is not the end, still more and more refinements to climate models and age uncertainties are being taking place to help anticipate the future climate trends with utmost accuracy.

1.3. Oceanography and climate of the study region:

The Arabian Sea is a unique basin composed of complex seafloor, seasonally changing hydrography, and isolation from the Arctic. It covers an area of about 3,863,000 km² and is located between 7° N and 25° N latitudes and 55° E and 75° E longitudes forming the northwest water body of the Indian Ocean (Figure 1). It is surrounded by landmasses to the west (Arabia), north (Pakistan) and east by coastal highlands (Deccan Mountains) of the western India. The basin is narrow in north and wide opens to the Indian Ocean in the south. Arabian Sea has one of the world's largest submarine fans viz., Indus Fan, formed by the sediments brought by the Indus River draining the Himalayas. Other major rivers, Narmada and Tapti join the Arabian Sea in the northern part of the west coast of India. Towards the south many small seasonal rivers draining the Deccan Mountains debouch considerable amount of fresh water and erosion products during the southwest (summer) monsoons. The Zuari-Mandovi drainage is one such river system that discharges in to the Eastern Arabian Sea (EAS) near the Goa province.

The Arabian Sea has several seafloor topographic features. Wide western continental shelf off India (a passive continental margin), narrow shelf off Oman, Owen Fracture Zone, Murray Ridge, and several seamounts. The most impressive geomorphologic feature of the Arabian Sea is the broad active Mid-Ocean Ridge system, which starts in Gulf of Aden and trends southwest as Carlsberg-Ridge, into an enechelon pattern of transform faults called Central Indian Ridge. The Carlsberg Ridge separates deep basin of Arabian Sea into two major sedimentary sub-basins: the Arabian Sea Basin and the Somali Basin. The Laxmi Basin in eastern part of the Arabian Sea bordering India has few conspicuous morphological features such as Raman, Panikker and Wadia seamounts (Bhattacharya et al., 1994).

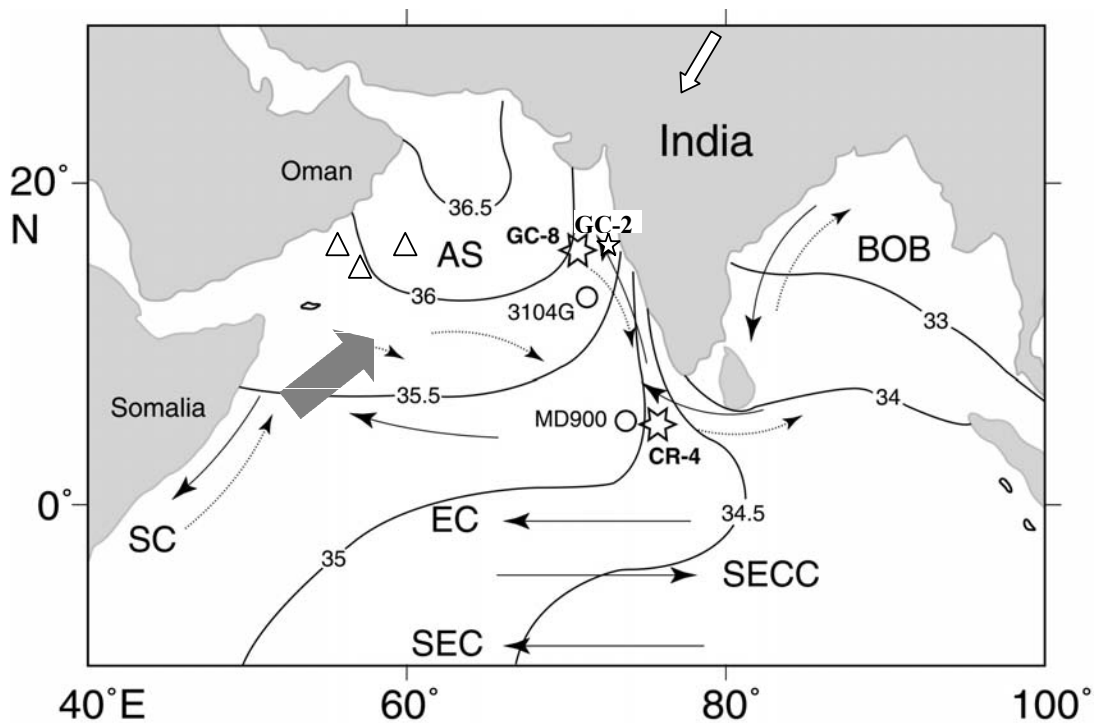


Figure 1: The northern Indian Ocean hydrography, monsoon system, and sediment core locations used in this study. AS is Arabian Sea and the eastern region of this basin (margin of India) is the present study area. BOB is the Bay of Bengal. The grey shaded thick box arrow indicates summer monsoon winds and open box arrow indicates winter monsoon winds. Continuous curved arrows are the winter monsoon surface water circulations and the broken arrows are the summer monsoon circulations. EC, SECC, and SEC are Equatorial Currents, South Equatorial Counter Currents, and the South Equatorial Currents respectively. The stars are the sediment cores used for the present study (SK117/GC02, SK117/GC08, and SK129/CR04; also see Table 1). Open triangles are the sediment cores studied for denitrification in the Oman region (Altabet et al., 1999), open circle with MD900 is the core studied by Rostek et al., (1993 & 1997) for palaeo-salinity and -SST reconstructions and 3104G is the core studied by Sarkar et al. (2000) for E-P reconstruction. The salinity contours are denoted with their salinity value. For details of circulation system and terminology see Shankar et al., (2002). There have been several palaeoclimate studies from the Arabian Sea, particularly in the western region, which are not shown in this figure to avoid crowding of the details.

Based on the depth profiles of salinity and potential temperature, Shetye et al., (1993) have identified three distinct water masses in the Arabian Sea, viz., Arabian Sea High Salinity Water (ASHSW), Red Sea Water (RSW), and Persian Gulf Water (PGW). The high salinity dense ASHSW forms in the northernmost Arabian Sea and spreads southwards within the upper 100 m of the mixed layer (Prasannakumar and Prasad, 1999). This water mass is the result of excess evaporation in the northern Arabian Sea. The PGW is located between ~200 m in the Gulf of Oman and ~400 m water depth further south. The PGW is derived from the overflow of Persian Gulf water into the Gulf of Oman over a sill depth of ~60 m and spreads into the Arabian Sea. The PGW loses its identity due to mixing with RSW as it moves southward. The RSW is the outflow from Red Sea over a sill depth of ~150 m. The high salinity RSW is located between ~500 m and ~800 m water depth (core occurs at ~600 m depth) and its southern extension could be traced up to 10° S latitude. The northern extension of the RSW is limited to ~18° N latitude (the comprehensive description of the Arabian Sea hydrography is available in You and Tomczak, 1993). The isolation and stagnation of the intermediate water and the lack of substantial horizontal advection together with very high productivity causes the development of intense Oxygen Minimum Zone (OMZ), which extends between 200 to 1200 m water depths (Wyrski, 1973; Olson et al., 1993). The core of the OMZ (< 0.5 ml O₂/L) is located around 600-800 m.

The Arabian Sea experiences extremes in both atmospheric forcing and oceanic circulation due to seasonally reversing monsoon wind system (Wyrski, 1973). During the northern hemisphere summer (May to August), solar radiations warm the land relatively faster than the ocean. As a result of this differential heating a steep pressure gradient is created between the low-pressure northern India-Tibet and high-pressure Equatorial Ocean. The dense oceanic air carrying moisture evaporated from the ocean move landward and subsequently curl towards the Indian

subcontinent causing heavy precipitation over the sea and Indian sub-continent known as the summer monsoon (Figure 1). With the onset of winter in November, both the land and the ocean lose heat by the radiation to space. The differential heat capacity of the land and ocean results in relatively greater cooling of the Indian subcontinent than the ocean resulting in cool dry winds to blow from the continent over the Arabian Sea, known as northeast monsoon during the winter (November-February) (Figure 1). The modern winter winds are significantly weaker than the summer winds (Shankar et al., 2002; Shetye et al., 1991) and hence their influence on the biogeochemistry of the Arabian Sea is believed to be low. The winter monsoon continues in a steady state until solar heating of the spring dissipates the temperature gradient that powers it. The development and evolution of these Indian seasonal monsoons are however much more complex.

The surface circulation in the Arabian Sea is modulated by the seasonal variation of the monsoon wind system. The seasonal reversals of the surface wind field over the tropical Indian Ocean are far more dramatic than in other regions of low latitudes, and these reversals have profound impact on the surface current system (Wyrki, 1973; Hasternath and Greishar, 1991). During the summer monsoon period the low level southeasterly trade winds of the southern hemisphere extend across the equator to become southerly or southwesterly in the northern hemisphere. The frictional stresses of the southwesterlies in turn drive the Somali current, which is a fastest open ocean current on the earth with a speed up to 7 knots (Smith et al., 1991; Shankar et al., 2002), the westward flowing south equatorial current, and the eastward flowing summer monsoon current (SMC). On the other hand, during the winter monsoon period, the oceanic circulation is relatively weak and is characterized by the north equatorial current (winter monsoon currents: WMC) and eastward flowing equatorial counter current. Thus, the direction of the wind-flow from the continent towards the Arabian Sea (in southwest direction) causes the circulation in the Arabian Sea to reverse (Figure 1).

The peculiar monsoon wind regime produces dramatic seasonal changes in physical and biogeochemical processes in the upper water column. Wind induced upwelling of nutrient rich water and related high primary productivity is one of the characteristics of this basin (Kabanova, 1968; Nair et al., 1989). High productivity and non-availability of well ventilated water to the intermediate depth result in the development of extremely low oxygen mid-depth layer causing intense denitrification (Naqvi, 1987), thus making the basin one of the worlds largest nitrogen sink (Codispoti, 1995). The formation of high salinity water in the northern Arabian Sea (Rochford, 1964; Morrison, 1997) due to excess evaporation-precipitation (E-P) (Cadet and Reverdin, 1981), and its seasonal spreading southward along the eastern region (Prasannakumar and Prasad, 1999) are unique seasonal hydrographic features of this basin. Therefore, the Arabian Sea is a complex but interesting natural laboratory to study the past climate. The western part of the Arabian Sea has attracted most of the attention of the palaeoclimatologists due to summer monsoon induced intense upwelling process in that region and proximity to the major desert land of Arabia. Where as, until recently other parts of the Arabian Sea were rather ignored. One of such areas is the EAS bordering the west coast of India. Hence, the present work aims to explore the responses of the highly dynamic EAS to the past climate change.

1.4. Study area:

The EAS comprises a dynamic water body receiving intense summer monsoon overhead precipitation with well-defined precipitation gradient from ~4000 mm in southern Konkan Coast to ~300 mm in northern Saurashtra Coast, decreasing northward at a rate of ~350 mm per degree latitude (Cadet and Reverdin, 1981; Sarkar et al., 2000). This region supports moderately high productivity due to seasonal upwelling (Haake et al., 1993; Sharma, 1977) and strong OMZ due to

which high export production is apparent (Rao and Veerayya, 2000 and references therein). In contrast to the large input of the dust to the western Arabian Sea from Arabia (Sirocko et al., 1991; Shimmield et al, 1990), the EAS receives very low dust input and is dominated by the terrigenous load delivered by the large network of rivers quickly draining the Deccan Mountains during the summer monsoon rains and to certain extent the Indus River input derived from the Himalayas particularly in the abyssal depths.

The surface salinity (hereafter only salinity) structure of the Arabian Sea is peculiar. The north to south decreasing, west to east trending isohalines of the basin are punctuated in the eastern region by the inflow of low salinity Bay of Bengal (BOB) water, which forms a low salinity tongue along the western margin of India (Figure 1). As such the basin-wide high salinity build-up due to excess E-P is largely compensated by the inflow of low salinity BOB water drawn by the WMC and its bifurcated arm known as poleward coastal current (PCC), thus maintaining the salt-balance (Prasad, 2001; Prasannakumar and Prasad, 1999). The summer monsoon dependency of the low-salinity water flow in to the EAS has been demonstrated (Shetye et al., 1991), and the details of the mechanism governing the low-salinity tongue are discussed in Chapter 6.1.

The biogeochemical responses of the Arabian Sea in general and western region in particular to the past climate and their linkage with monsoon variations have been traced in the sediment. Therefore, the sedimentary records from the EAS are well-suited repository to explore the fluctuations in closely interlinked past monsoon strength, salinity structure, productivity, and fluvial erosion in Deccan Mountain region. As the eastern region is the least studied region of the Arabian Sea in regard to palaeoclimate reconstruction, may be holding interesting information with respect to the biogeochemical responses associated with the climate change.

1.5. Previous study:

The Indian monsoon system is one of the major atmospheric components of the tropical climate and is a complex system. Previous studies have suggested that the strength of the summer monsoon, upwelling, and productivity in the Arabian Sea are all coupled together. Those investigations were mainly concentrated in the western Arabian Sea, especially in the summer monsoon driven upwelling cell of the Oman Margin. The oxygen isotopes have been extensively used to understand the past changes in the Indian Monsoons.

The oxygen isotope ratio of the biogenic calcite has been the most reliable tool for the palaeo-climate and monsoon reconstruction. The oxygen isotopic composition of calcareous fossils depends upon the isotopic composition of the contemporary ambient water, which in turn depends upon the local salinity and sea surface temperature (SST). The vital-, size- and dissolution-effects affecting the isotopic composition of the calcite tests (Dogde, et al., 1983; Duplessy et al., 1981) may be ignored because the former can be assumed to have uniform effect through time and the latter two problems can be circumvented by careful selection of the sample site (well above carbonate lysocline) and intact specimen from a narrow size-range. In the EAS the salinity depends largely upon the E-P balance and BOB water influx. Where as, the SST in the region depends upon monsoon wind regime and the coastal upwelling. Therefore, the calcite tests of the planktonic foraminifera from sediment cores have been the ideal proxy for understanding the past changes in complex interaction of the E-P, water mass characters, circulation, and monsoon strength (Prell et al., 1980; 1984a, 1984b; Duplessy, 1982; Sarkar et al., 1990; Sirocko et al., 1993; 1996) specific to this study area.

The planktonic foraminifera oxygen isotope based studies from the Arabian Sea have indicated that the strength of summer monsoons has varied greatly during the late Quaternary (Prell., 1978; Prell et al., 1980; Prell., 1983; Niitsuma et al., 1991; Spaulding and Oba, 1992). The studies using ODP sediment cores have shown

significant variations in summer monsoon and its effect on oceanic productivity in the Western Arabian Sea (Shimmield et al., 1990). It is believed that the Indian summer monsoon around 9 Ka were intense than during the LGP (24-11 Ka) based on large scale climate models and the past-upwelling records (Clemens and Prell., 1990; Sirocko et al., 1993; 1996; Naidu., 1995). The Holocene E-P balance reconstruction for the EAS by Sarkar et al., (2000) has indicated a steadily increased summer monsoon precipitation since the ~10 Ka up to ~2 Ka. This Holocene summer monsoon trend however does not agree with the summer monsoon variations in the western region recorded by upwelling indicator species (Naidu and Malmgren, 1995). Based on the $\delta^{18}\text{O}$ of *G. ruber* from both the Arabian Sea and BOB, Duplessy (1982) suggested that the basin-wide LGM-SSTs were nearly similar to or even slightly warmer than the Holocene. Hence, he assumed that the Holocene-LGM $\delta^{18}\text{O}_{G.ruber}$ contrast was solely due to the variation of the salinity in the region. The global circulation models, taking in to account various climatic parameters for Glacial-Holocene boundary conditions suggested that the Indian summer monsoon intensity variation was largely forced by the E-P accounting for ~23 % of the total forcing factor (Prell and Kutzbach, 1992). In contrast to the Duplessy's (1982) assumption, the alkenone based SST reconstructions indicated 2° - 3° C lowered SST in the LGM-EAS (Cayre and Bard, 1999; Rostek et al., 1997; Sonzogni et al., 1998). Similar drop in SST has been recorded in the LGM sections of the tropical South China Sea sediment cores (Kienast et al., 2001). Thus it appears that the LGM-SSTs in the low latitude regions in fact were lower than the Holocene. However, the magnitude of SST-lowering during the LGM was much smaller than in the high latitude regions (Ikehara et al., 1997).

Presently high surface productivity and subsequent oxidation of settling organic matter consumes large amount of dissolved oxygen at low oxygenated intermediate water leading to an exceptionally broad and stable mid-water OMZ in

the region (Olson et al., 1993). High content of organic carbon in surface sediments in the EAS, especially western continental margin of India suggest high export production and better preservation (Calvert et al., 1996; Paropkari et al., 1992; Slater and Kroopnick, 1984; Rao and Veerayya, 2000). The primary cause of carbon enrichment in sediment has been previously debated (Paropkari et al., 1987; 1992 and references therein). The pre-existing deep-water anoxic condition (Calvert et al., 1993; Demaison and Moore, 1980; Paropkari et al., 1992), high productivity and favourable sediment texture (Calvert et al., 1995; Pederson and Calvert, 1990; Pederson et al., 1992; Rao and Veerayya, 2000) have been invoked as the causes for good preservation of the carbon in the EAS sediment. Further details are out of the scope of this study. Recent studies however have suggested that the inherent low oxygen character of the feed-water at intermediate depth not only sustains the OMZ (Olson et al, 1993), but also contributes to the preservation of organic carbon (Schulte et al., 1999 and references therein). Irrespective of the debate on carbon inventory of the Arabian Sea sediment, the sedimentary organic matter has been extensively used to understand the past-productivity variations in the basin.

Interestingly, there have been contrasting views with respect to past productivity in the Arabian Sea, which is dealt in detail in Section 6.3. Here it is worth mentioning that the past productivity changes in the basin have exhibited region specific (western versus eastern) responses to the climate change. On one hand, the western Arabian Sea has been shown to record interglacial high productivity (Emeis et al., 1995; Naidu and Malmgren, 1996; Shimmeild et al., 1990; Spaulding and Oba, 1992), while on the other hand, biomarkers and sedimentary organic carbon have indicated enhanced glacial productivity in the EAS (Cayre and Bard, 1999; Rostek et al., 1997; Schulte et al., 1999; Thamban et al., 2001). The observations indicating stronger winter monsoons during the LGM than the Holocene (see Duplessy, 1982) has been the nodal point for the hypothesis invoking glacial high productivity; where

as, the summer monsoon driven intense basin-wide upwelling has been the central cause for interglacial high productivity.

Thus the EAS appears to be an intriguing region with respect to its response to the past climate driven monsoon variations. Hence, it is necessary to explore this region in detail to understand the effects of past climate on relative strength of the monsoons and associated responses such as productivity, fluvial input of detritus, hydrography, denitrification etc. Did these parameters in the EAS responded in concert with each other as a coupled responses to the varying monsoon regime or were they decoupled responses for a given climatic scenario needs to be addressed using multi-proxy approach, and forms the theme of the present investigation.

2. Objectives of the present study

For the present study, it is proposed to investigate the linkage between past variations in the Indian monsoon system and its effect on the photic zone productivity, local hydrography, and fluvial input in the EAS utilizing a multi-proxy approach. The following causal relationships need to be explored to achieve that objective.

- a) The past variations in the relative intensity of the Indian monsoons by tracking the relative changes in E-P and coastal circulation using planktonic foraminifera- $\delta^{18}\text{O}$ and available alkenone-SST patterns from the region. Both the high-resolution Holocene-Glacial and low-resolution glacial-interglacial time slices would help in reconstruction of the past monsoon variations.
- b) The fluvial silicate-detritus distribution in the sediment column deposited on the continental shelf, in the vicinity of any Deccan Mountain Rivers is expected to produce characteristic signals in concert with the summer monsoon intensity. Because, the Deccan Mountain Rivers are dependent upon the summer-monsoon and are exclusively seasonal. Therefore, the down-core variations of specific size detrital grain ratios may be able to provide important clues about the variations in summer monsoon rains.
- c) There is a large volume of work on record showing strong relationship between upwelling, productivity, and the summer monsoon intensity particularly from the western Arabian Sea. If the summer monsoons were solely responsible for driving the productivity in the Arabian Sea, then the proxies such as biogenic-calcite, organic-matter, and scavenged-Al from the EAS also are expected to produce overlapping signals in concert with the past summer monsoons.

d) The high productivity and low oxygen characteristic intermediate water maintain intense modern-OMZ in the Arabian Sea. The past variation in the OMZ intensity could be evaluated through variation in water column denitrification recorded by the sedimentary nitrogen-isotopes. The past changes in denitrification intensity may be a useful tool to understand the variation in monsoon intensity (*vis-à-vis* productivity) and intermediate water hydrography.

Three gravity cores representing three different depositional environments in the EAS were selected for the present work from the collection of the National Institute of Oceanography (see Figure 1 & Table 1). Due to certain analytical constraints it was not possible to generate strictly paired data for the studied cores, and hence the interpolation technique was used to evolve common time-scale for different variables wherever required. The chronology for Holocene-LGP sections of the cores may contain certain uncertainty due to the non-availability of AMS-¹⁴C dates. I have rigorously assessed the structure of the oxygen isotope profiles while evolving age models; however, refrain from discussing several subtle fluctuations in view of the above chronological limitation particularly for the Holocene-LGM section.

3. Material

Sediment cores selected for the present study are from the ORV. Sagar Kanya cruise-117 (SK-117: October 1996) and -129 (SK-129: December 1997). Two cores were from the central-EAS off Goa (SK-117 collection) and one core was from the southern-EAS (SK-129 collection). For convenience I refer the former core locations as 'northern region' and the latter core location as the 'southern region' of the EAS. The core-tops of the selected sediment cores were assumed to be intact as evident by fluffy upper layer and the cores do not contain any indications of slumping or turbidite. The cores were sub-sampled on board at 2 cm intervals after scraping-off about half a cm outer layer to eliminate any contamination caused due to mixing of younger and older sediment when the corer penetrates into the sediment column. The sub-samples were transferred to clean and labelled polyethylene bags, sealed and stored in labelled plastic bottles.

The relevant details of the samples are given in Table 1 and their locations in Figures 1. The core SK-117/GC-02 is from the continental shelf region ($15^{\circ} 28. 96' N$ and $72^{\circ} 50. 72' E$, water depth 226 m), ~150 km off from the discharge point of two Deccan Rivers viz., Mandovi and Zuari flowing through the State of Goa. Therefore, this core is expected to record continental detritus-input signals generated by the variation in the intensity of those rivers. The preliminary microscopic observations indicated that a significant portion of the coarse fraction indeed contain abundant detrital grains, thus providing an opportunity to quantify the variations in terrigenous supply. The core SK-117/GC-08 ($15^{\circ} 29. 71' N$ and $71^{\circ} 00. 98' E$, water depth 2500 m) was located on the continental slope region off the GC-02 core. This location falls within the seasonally varying modern-ASHSW front (Prasannakumar and Prasad, 1999; Prasad, 2001) and should be able to provide a record of the past changes in the intensity and spreading of that northern Arabian Sea origin ASHSW high salinity water mass. The core SK-129/CR-04 ($6^{\circ} 29. 67' N$ and $75^{\circ} 58. 68' E$, water depth

2000 m) on the other hand was located below the modern WMC, which advect low BOB water in to the Arabian Sea. Therefore, this core in combination with the GC08 may be able to provide a record of variation in the strength of WMC and EAS-characteristic PCC (Shetye et al., 1991). The two deep-water cores (SK117-GC08 and SK129-CR04) are also expected to provide information on relative changes in the past salinity-balance in the EAS, because, the modern salinity budget of the Arabian Sea is largely governed by the monsoon currents (see Prasannakumar and Prasad, 1999; Shankar et al., 2002). Apart from these specific potentials, the cores must have preserved the past records of climate driven changes in marine productivity. Thus the material selected for the present study has a potential for a comprehensive understanding of the monsoon and biogeochemical response of the EAS to the past climate.

Table 1. Details of samples used in the present work.

Core	Latitude (N)	Longitude (E)	Water-depth (m)	Core length (cm)	Type of the sediment
SK117-GC-02	15° 28. 96'	72° 50. 72'	226	390	Carbonate ooze. Shell fragments and silicate grains occur within the carbonate and silt matrix.
SK117-GC-08	15° 29. 71'	71° 00. 98'	2500	408	Carbonate ooze intermixed with clay and silt material. The YTT* characteristic glass-shards are abundant at ~290 cm depth in core.
SK129-CR-04	06° 29. 67'	75° 58. 68'	2000	504	Carbonate ooze intermixed with clay and silt material. The YTT* characteristic glass-shards are abundant at ~220 cm depth in core.

(*YTT = Youngest Toba Tuff originated from the Indonesian Archipelago volcanism has been dated to be ~72 Ka (Ninkovitch,1978). This tuff has been shown to have transported by winds across the Arabian Sea up to Arabia (Rose and Chesner,1987); across the equator in to the southern hemisphere (Pattan et al., 1999); and even up to the Greenland (Zielinski et al., 1996). The extension of the YTT into Greenland indicates the intensity of the eruption. Several researchers have used this volcanic tuff as an excellent tie-point for oxygen-isotopic chronology of the sediment cores. Similarly the presence of YTT in two cores for present study has provided excellent tie-point for establishing the isotope chronology. (**Hereafter the above sediment cores are referred as GC02, GC08, and CR04 respectively**).

4. Methods

The optimum numbers of representative samples from different marine setting in the EAS have been used for obtaining the required proxy-data. The data acquisition techniques and working principles of analytical tools utilized for the study are briefly described in this section. The proxies used are:

1. Planktonic foraminifera-calcite oxygen isotopes for chronological framework and to understand E-P changes in response to monsoon fluctuation and past variation in the salinity adjustment in the region.
2. Planktonic foraminifera-calcite carbon-isotopes, organic carbon and its carbon-isotopes, sedimentary-nitrogen and its isotopes, and carbonate fluxes for reconstructing the past variation in productivity and OMZ intensity in the region.
3. Sediment texture and grain-size variation to understand the changes in the intensity of fluvial erosion in the Deccan Mountain region.
4. Alkenone unsaturation index to confirm the previously reported SST-shift from the LGM to Holocene.
5. Particle scavenged-Al and -Mn for independently testing the productivity changes.

It is worthwhile to note that the above parameters in modern climate setting are related directly or indirectly to the Indian monsoon intensity. My effort therefore would be to understand interlink between those oceanic responses and the past climate fluctuation in general during the late Quaternary, and in particular from the immediate past Glacial to the present Holocene period. The previous studies have also indicated that the Indian monsoon system and the Arabian Sea responses to the monsoons provide important feedback for the global carbon dioxide cycling (Overpeck et al., 1996; Schulz et al., 1998). Even though the present study is not

aimed at carbon dioxide issue, but may provide at least partly explanations for its glacial-interglacial changes.

4.1. Sediment texture analysis:

The proportion of sand, silt, and clay fractions in the sediment was quantified using standard sedimentological techniques such as wet sieving and pipette analysis. The pipette analysis is based on the Stoke's law of settling velocity (Folk, 1968). The Stoke's Law is defined as ' $V=CD^2$ ', where V is the settling velocity (cm/sec) of a particle, C is the constant defined by the viscosity of settling medium and the density of the settling particles, and D is the particle diameter (cm) assuming settling particle as a sphere. The obtained proportions (in weight percent) of the fractions were used to define the sediment texture following Pettijohn et al., (1972) classification.

The raw sediment was rinsed twice with RO-water (reverse osmosis treated) to remove the salts and dried at $\sim 50^{\circ}\text{C}$. The dried salt-free sediment was weighed accurately (10-15 grams) and transferred to clean beaker. The weighed sample was soaked in 50 ml of RO-water and was dispersed with 10 ml of 10 % sodium hexametaphosphate. The sample was stirred gently after every 20 minutes for 4 hours to achieve complete dispersion of fine fraction. The dispersed sediment sample was wet sieved through 230-mesh ($63\ \mu\text{m}$) sieve in a soft jet of RO-water. The $-63\ \mu\text{m}$ fraction was collected in a clean 1000 ml measuring cylinder. Sufficient care was taken to limit the washing volume to $< 1000\ \text{ml}$. The volume was finally made to 1000 ml before starting the pipette analysis.

The $+63\ \mu\text{m}$ fraction (sand) retained on the sieve was transferred to a pre-weighed 50 ml beaker, dried at $\sim 80^{\circ}\ \text{C}$, and weighed. The $-63\ \mu\text{m}$ fraction (clay + silt) in the measuring cylinder was subjected to pipette analysis. The $-63\ \mu\text{m}$ fraction was stirred vigorously with the help of a perforated disc-stirrer for about 2 minutes. The

time is noted down soon after the stirring is stopped. A 100 ml of settling mixture containing clay fraction was pipetted from designated depth-level in the cylinder at defined time-intervals depending upon the ambient temperature of the settling medium. The clay fraction was transferred to pre-weighed beakers and dried at ~50°C. The dried clay fraction was weighed and stored in the plastic vials for the further analysis. The weight of the clay fraction was corrected for the weight of dispersant. The weights of clay and sand fractions were subtracted from the original weight of the sample to obtain the silt content. Further, the weight each fraction was translated in to percent proportion. Several duplicate samples were also analysed to assess the precision of the results, which is within $\pm 3 \%$.

4.2. Sediment grain-size measurement:

The continental shelf core GC-02 was analysed for detailed grain-size distribution using a Malvern Mastersizer-2000 Laser Particle Analyser. The Mastersizer basically works on the Fraunhofer model and Mie theory. The former can predict the scattering pattern that is created when a solid opaque disc of known size is passed through a laser beam, while the latter theory predicts the way the light is scattered by spherical particles. But in nature the particles are not regular as considered by the above fundamental models. However, the key point here is that, if the size of a particle and other details of its structure are known, one can predict the way it scatters the light. In other words, each particle has its characteristic scattering pattern that is different than any other size particles. The Mastersizer works precisely backwards on the above theory. It actually captures the scattering pattern from a field of particles passing through a laser beam and calculates the sizes of the particles responsible for creating characteristic scattering patterns.

As particle size proxy was required to monitor the changes in detrital grain input from the fluvial activity, it is necessary to remove the carbonate skeletons from

the sediment. Therefore, the sediment was completely decarbonised in mild HCl (0.5 N), washed repeatedly with RO-water to remove the traces of acid, dispersed in an ultrasonic bath and fed to the optical unit of the Mastersizer. The detector array of the Mastersizer takes several snap-shots of scattering produced by the particles settling through the analyser beam at particular time. The inbuilt Malvern software converts the scattering pattern in to the volume concentration using Beer-Lambert Law and expressed as percent. The volume percentages are used for interpretations without any conversions because the aim is to monitor relative variation of specific size-band particles rather than quantifying them for absolute grain-size distribution. The replicate measurements of few random samples suggest that the precision of the results is within $\pm 1\%$ of the distribution volume of a given size-band.

4.3. Calcium carbonate analysis

In the regions away from the hydrothermal activity and atmospheric dust sources, the sedimentary carbonate is normally derived from calcite secreting planktonic organisms. The areas in the vicinity of river discharge contain significant amount of continental silicate detritus. Hence, the down-core variation of these components provide first hand information about the past productivity and river intensity, which in turn are dependent upon the summer monsoon strength in the EAS. Therefore, the accumulation rate (flux) of biogenic calcite is a useful tool to assess the past productivity because it minimises the bias due to dilution by the terrigenous material and variations in sedimentation rates. The dried and accurately weighed salt-free sediment was reacted with 0.1 N HCl until the complete evolution of the CO_2 . The leachate was centrifuged and decanted in to volumetric flask and diluted with 18 mohm deionised water. The diluted solution was analysed for Calcium (Ca) in a Perkin-Elmer® OPTIMA-2000 DV ICP-OES. The measured Ca was translated in to CaCO_3 using a conversion factor of 2.497. The accuracy of the measurement was assessed by analysing AR-grade synthetic CaCO_3 powder

treated in the same way as the samples. The duplicate measurements of the sample leachates and the synthetic-CaCO₃ standard suggested that the analytical precision was within ±1 % and the accuracy was within ±2 %. The same leachates were also used for analysing Aluminum (Al). There is a possibility of HCl leaching the clay particles in the sediment. However, there are no reports demonstrating the corrosive effect of very mild-HCl on the clays. Therefore, I assume that the strength of the acid used (0.1 N HCl) for carbonate dissolution is the optimum strength to leach-out the carbonate and particle scavenged metals from the water column leaving behind the clays unaffected (see Banakar et al., 1998).

4.4. Sedimentary stable isotope analysis

4.4.1. Calcite oxygen- and carbon-isotopes:

Oxygen has three naturally occurring stable isotopes, ¹⁶O (abundance 99.763 %), ¹⁷O (abundance 0.0375 %) and ¹⁸O (abundance 0.1995 %). Because of the higher abundance and the greater mass difference, the ¹⁸O/¹⁶O ratio is normally determined, which may vary in natural samples by about 10% or in absolute numbers from about 1:475 to 1: 525. As a result of fractionation during evaporation, the vapour tends to enrich with H₂¹⁶O relative to H₂¹⁸O leaving the reservoir (ocean) enriched with H₂¹⁸O. When water vapour condenses to produce precipitation the fractionation is in the opposite sense, i.e., the water condensing from vapour and then precipitating is enriched with H₂¹⁸O relative to the remaining vapour. Hence, the first condensed rain is more enriched with H₂¹⁸O than the later rains. The greatest fractionation is however evident during the evaporation. Thus, the atmospheric evaporation-precipitation cycle results in net fractionation of oxygen isotopes and precipitated water is richer in H₂¹⁶O than the seawater from which it was evaporated. On a global scale, when ¹⁶O-enriched water vapour is precipitated as snow and builds up to form glaciers and ice-caps, then the oceans will have lost proportional

amount of ^{16}O along with fresh water until the ^{16}O enriched water locked in continental ice is released back to the ocean by melting. Therefore, the $^{18}\text{O}/^{16}\text{O}$ of the ocean produce distinct responses to the climate change. In other words the global oceans are ought to exhibit higher $^{18}\text{O}/^{16}\text{O}$ during the cold and dry glacial climate when the continental ice has waxed to a greater extent (more than 29% during the last glacial period compared to modern extent), and during the warm and humid interglacial climate the global oceans are replenished with ^{16}O due to waning of the ice sheets that have locked-in fractionated lighter- ^{16}O from the ocean water. Such relative variations in the seawater $^{18}\text{O}/^{16}\text{O}$ ratios (higher during glacial periods and lower during interglacial periods) are preserved globally in the contemporary calcite skeletons secreted by the marine organisms such as foraminifera. In spite of large variation in absolute values of the $^{18}\text{O}/^{16}\text{O}$ exhibited by different species of the foraminifera depending on vital effects and their habitat, the general structure of the time-series calcite- $^{18}\text{O}/^{16}\text{O}$ in the sedimentary records over the world oceans is remarkably similar. This similarity rather suggests not only the global nature of the past climate change but also indicates the fidelity of the marine planktonic organisms to record such changes.

Carbon occurs in nature as highly reduced organic compounds in the biosphere to highly oxidized inorganic compounds such as CO_2 and carbonates. It comprise of two stable isotopes ^{12}C (natural abundance of 98.89%) and ^{13}C (natural abundance of 1.11%). The global seawater distribution of carbon-isotopic composition ($\delta^{13}\text{C}$) reflects the nutrient content and the marine photosynthesis (Kroopnick, 1985). The inter-oceanic thermohaline circulation (Broecker, 1991) is believed to convey the North Atlantic Deep-Water (NADW) and Antarctic Bottom-Water (AABW) $\delta^{13}\text{C}$ characters across the global oceans through overturning. However, in the surface ocean the source water $\delta^{13}\text{C}$ characteristics are modified to a greater extent due to ageing as it travels away from the source region and mixing

with local water masses. The past climatic fluctuations in fact have affected the production of deep-water masses and hence the reservoir $\delta^{13}\text{C}$ composition, the details are out of the scope of the present study. Here, only the application of $\delta^{13}\text{C}$ in sedimentary biogenic material with respect to changes in local productivity is considered.

The carbon-isotopic fractionation basically is the result of both thermodynamic and kinetic processes acting simultaneously within the marine reservoir. In case of inorganic carbon associating with secretion of carbonate skeletons, the fractionation mechanism is by isotope equilibrium exchange reactions, which leads to enrichment of ^{13}C in carbonate. In organic matter, it is by the process of kinetic isotope effects i.e., during photosynthesis the light isotope ^{12}C concentrates in the synthesized organic matter leaving the ambient water enriched with ^{13}C . In other words, during high productivity episodes, the organic matter exhibits enrichment of light carbon and therefore, contemporary inorganic calcite secreted by the organisms from ^{13}C enriched ambient water should therefore exhibit relative enrichment of heavy carbon. The main isotope-discriminating steps during biological carbon fixation are 1) the uptake and intracellular diffusion of CO_2 and, 2) the biosynthesis of cellular components. The comprehensive details of the isotopes used for the present study are available in Hoefs (1997).

For the measurement of calcite carbon and oxygen isotope ratios, upper mixed layer dwelling planktonic foraminifera *Globigerinoides sacculifer* (*G. sacculifer*) (<30 m: Hemleben et al., 1989; Chaisson and Revello, 2000) was selected. Since the objective of the present work is related with the surface ocean processes and responses, this species is well suited. About 30-40 clean individuals of 250-350 μm size were picked under a binocular microscope from the coarse fraction (+63 μm) of the sediment sections. The tests were carefully observed under the microscope to avoid damaged specimen due to dissolution and specimen with terminal sacs. As the

terminal sacs develop at deeper depths during their gametogenesis, the specimen with such sacs therefore may alter the surface water isotopic signals by contaminating with heavy-oxygen enriched signals inherent to colder deep ambient water (Hemelben et al., 1989). The sac-free specimen were transferred to thimbles, mildly crushed with a blunt pin in presence of a drop of ethanol to break-open the chambers, sonicated to remove fine detritus and dried at 50°C. The thimbles were placed in the numbered disc-holder of the reaction vessel, which was maintained under vacuum and connected to a glass transfer line having three cold fingers for three-step CO₂ purification.

The *G.sacculifer* tests were allowed to react completely in reaction vessel containing 100 % Phosphoric Acid maintained at 60° ± 1° C. The CO₂ released during the reaction ((3CaCO₃ + 2H₃PO₄ ⇒ 3CO₂↑+ 3H₂O + Ca₃(PO₄)₂)) was purified thrice in the glass line maintained under vacuum. The liquid-nitrogen and a mixture of liquid-nitrogen and ethanol (to obtain solution having ~ -105° C temperature) were used respectively to trap moisture in cold-fingers and release only the CO₂. The purified CO₂ was analysed for oxygen- and carbon-isotopic ratios using a Finnigan MAT-251® mass-spectrometer. The measurement of ¹⁸O/¹⁶O and ¹³C/¹²C is done by using mass discriminator at 46 and 45 respectively against reference standard NBS-20 calibrated with PDB. The final isotopic ratios are expressed in PDB-calibrated scale (Table 2).

Table 2. Standards used for expressing isotopic compositions

Element	Description of standard	Standard
Calcite-O & C	<i>Belemnitella americana</i> from the	PDB
Organic matter-C	Cretaceous Peedee formation, South Carolina	
Sedimentary-N	Air nitrogen	AIR

The stability of the equipment was obtained by repeatedly analysing an in-house standard Solenhoffen Limestone over the analytical period of three months (June-August, 2001) and the results were accurate and precise within ± 0.02 ‰ (Table 3).

Table 3: Isotopic measurement results of the in-house Reference Standard (Solenhofen Limestone)

Sl. No.	$\delta^{18}\text{O}$ ‰ vs PDB	$\delta^{13}\text{C}$ ‰ vs PDB
1	-4.035 ± 0.011	-4.049 ± 0.012
2	-4.101 ± 0.011	-4.162 ± 0.009
3	-4.129 ± 0.018	-4.223 ± 0.012
4	-4.023 ± 0.016	-4.018 ± 0.008
5	-4.140 ± 0.018	-4.224 ± 0.015
6	-4.027 ± 0.021	-4.047 ± 0.013
7	-4.140 ± 0.015	-4.189 ± 0.008
8	-4.100 ± 0.028	-4.068 ± 0.011
9	-4.130 ± 0.015	-4.162 ± 0.016
10	-4.129 ± 0.023	-4.201 ± 0.008
11	-4.158 ± 0.020	-4.136 ± 0.015
12	-4.126 ± 0.012	-4.152 ± 0.017
13	-4.047 ± 0.014	-4.099 ± 0.003
14	-4.111 ± 0.019	-4.204 ± 0.009
15	-4.027 ± 0.029	-4.170 ± 0.009
16	-4.094 ± 0.034	-4.140 ± 0.009
17	-3.967 ± 0.026	-4.039 ± 0.014
18	-4.118 ± 0.024	-4.162 ± 0.007
19	-4.122 ± 0.035	-4.132 ± 0.014
20	-4.091 ± 0.028	-4.091 ± 0.015
21	-4.080 ± 0.012	-4.072 ± 0.012
Average:	-4.090 ± 0.020	-4.130 ± 0.011

4.4.2. Organic matter and carbon- and nitrogen- isotopes:

The different photosynthetic pathways distinctly fractionate C-isotopes, and the nitrogen fixation-denitrification processes leave distinct signals of nitrogen-isotopes in the sedimentary organic matter (Wada and Hattori, 1978). Therefore, it is possible to understand the past variation in organic production and its fate during oxidation and burial by studying the sedimentary organic matter. As such the organic carbon (C_{org}) and C/N ratios together provide fairly accurate information about the marine productivity, if the organic matter has escaped diagenetic alterations in the water column during its export to the seafloor or after burial in to the sediment. Therefore, well-preserved organic matter (normally evident by moderate to high organic carbon content in sediment) can be a measure of the photic zone productivity. The Redfield ratios of C/N are useful to evaluate the contribution of terrestrial organic matter in the marine sediment (Peters et al., 1978). The marine sedimentary biomarkers such as alkenones (di-, tri- and tetra-unsaturated ethyl and methyl ketones) are proved to be reliable indicators of marine productivity (Ikehara et al., 2000), as they are refractory to the settling or burial diagenesis unlike organic carbon (Brassell, 1993). Keeping this potential in mind, one core (GC-08) was subjected to detailed measurement of organic components and their isotopes to reconstruct the past climate driven productivity and OMZ-variations.

The finely powdered (-250 μ m) bulk sediment was decarbonised with 1 N HCl until carbonate fraction was removed quantitatively. The decarbonised fraction was washed repeatedly with de-ionised water to remove the traces of acid. The carbonate-free fraction was dried at 60°C. Accurately weighed dried sediment fraction was analysed for C_{org} and N in Fison® NA-1500 Elemental Analyser. The C- and N-isotopes were also measured simultaneously by flow-injection method using online Finnigan® MAT252 mass-spectrometer after combusting the sample and converting particulate-C and -N in to their gaseous components. The results of

isotopic ratios are expressed as PDB calibrated units for C-isotopes and atmospheric-N₂ calibrated units for N-isotopes (Table 2). The accuracy of the results as obtained by repeated measurement of amino acid reagents and reference standards are within $\pm 2\%$ for C- and N-contents and within $\pm 0.2\text{ ‰}$ for C- and N-isotopes.

4.4.3. Alkenone extraction and measurement:

Alkenones forms a family of temperature-sensitive lipids comprising a series of C₃₇-C₃₉ di-, tri-, and tetra-unsaturated ethyl- and methyl-ketones synthesised by the *Prymnesiophyceae* group of unicellular coccolithophorid algae, particularly *Emiliana huxleyi* species in the mixed layer (Volkman et al., 1980). These organic compounds are highly refractory to the diagenesis during or after their export to the seafloor. Additionally, the unsaturation index of the alkenones was found to be sensitive to the ambient water temperature at which they are synthesised. These properties rendered the alkenones as potential proxy for both SST and marine productivity see Brassell, 1993; Prahl et al., 1998; Yamamoto et al., 2000). In the recent past several researchers have used the alkenones extensively in palaeoclimate studies (see Cayre and Bard, 1999 and references therein).

Accurately weighed fine powders of dried sediment (1-2 grams) were taken in centrifuge tubes and the organic molecules were extracted in Dichloromethane-Methyl alcohol mixture under sonification. The extracted molecules were subjected to chromatographic separation of alkenones following the methods described by Yamamoto et al. (2000). Exactly 50 μl of internal standard (C₃₆H₇₄) containing 0.05 g/l of C₃₆ to yield 5 ng in the eluted alkenone fraction was used as spike. The third (toluene eluted) fraction containing alkenones and internal standard were dried under nitrogen stream and the residue dissolved in ultrapure hexane, transferred to collapsible vials, loaded on the autosampler and analysed on a Hewlett-Packard®

Gas-Chromatograph. The results of the measurement compared to an in-house standard are within $\pm 3\%$. The sum of di- and tri- ethyl and methyl ketones (Σ alkenones) is considered here as the proxy for productivity. The unsaturation index (U_{37}^k) was calculated from the concentration of di- and tri-unsaturated alkenones using Brassell et al. (1986) equation: $[C37:2MK]/([C37:2MK]+[C37:3MK])$. The SST was then obtained using the calibration of Prah et al. (1988):

$$U_{37}^k = 0.034T + 0.039, \text{ where } T \text{ is the SST in } ^\circ\text{C}.$$

4.5. Estimation of excess- Al and -Mn:

The sedimentary scavenged-Al may be useful to support the other productivity proxy data, and particulate Mn-oxide is useful in understanding the redox conditions of the water. The details of particle scavenged-Mn and -Al and their potential application in marine geochemical processes are available in Banakar et al. (1998); Dickens and Owen (1994); Murray and Leinen (1993). The scavenged elements can be estimated from bulk sediment composition by subtracting the detrital silicate bound contents (Murray and Leinen, 1993; Banakar et al., 1998). However, extremely mild acid leaching can extract the particle surface bound and authigenic oxide bound scavenged metals from the bulk sediment providing an opportunity of direct measurement such scavenged phases of metals from seawater.

The 0.1 N HCl leached fraction from the bulk sediment (used for carbonate measurement) was utilized to estimate the excess-Al and -Mn content. A Perkin-Elmer® Optima DV-2000 ICP-OES was used for the analysis following three point calibration obtained by multi-element standards of Sigma-Aldrich®. A synthetic standard was prepared for estimation of accuracy and precision of the results. The analysed results are accurate and precise within $\pm 3\%$.